Spinodal Decomposition in High Temperature Gauge Theories

Travis R. Miller and Michael C. Ogilvie

Department of Physics, Washington University, St. Louis, MO 63130

October 31, 2018

After a rapid increase in temperature across the deconfinement temperature T_d, pure gauge theories exhibit unstable long wavelength fluctuations in the approach to equilibrium. This phenomenon is analogous to spinodal decomposition observed in condensed matter physics, and also seen in models of disordered chiral condensate formation. At high temperature, the unstable modes occur only in the range $0 \leq k \leq k_c$, where k_c is on the order of the Debye screening mass m_D. Equilibration always occurs via spinodal decomposition for $SU(2)$ at temperatures $T > T_d$ and for $SU(3)$ for $T \gg T_d$. For $SU(3)$ at temperatures $T \gtrsim T_d$, nucleation may replace spinodal decomposition as the dominant equilibration mechanism. Monte Carlo simulations of $SU(2)$ lattice gauge theory exhibit the predicted phenomena. The observed value of k_c is in reasonable agreement with a value predicted from previous lattice measurements of m_D.

PACS numbers: 12.38.Mh, 11.10.Wx, 11.15.Ha, 12.38.Gc

Typeset Using *REVTEX*

I. INTRODUCTION

In a heavy ion collision, changes in local energy densities of 1 GeV/fm^3 and higher occur on a time scale less than 1 fm/c. During the initial stages of the formation of a quark-gluon plasma, the system is thermodynamically unstable. Some consequences of this instability can be studied with both simulation and analytical techniques. In particular, we find the existence of exponentially growing long wavelength modes in the approach to equilibrium. Such behavior is referred to as spindodal decomposition in condensed matter physics. [1] [2] We will study spinodal decomposition in finite temperature gauge theories using both analytical and simulation techniques. The existence of exponentially growing long wavelength modes cutoff at a fixed wavelength depends only on the features of the equilibrium effective action in an unstable region. Although the methods we use are not based on the true real-time evolution of the system, they give a consistent picture of some basic features of real-time behavior.

We consider first the generic case of a pure $SU(N)$ gauge theory in which the temperature is raised rapidly from a temperature less than T_d, the deconfinement temperature, to a temperature above T_d. We refer to such a rapid increase in system temperature as a quench; this nomenclature is borrowed from statistical mechanics, where it is usually applied to rapid cooling of a system below a critical temperature. It is appropriate here because it is the high temperature phase of the pure $SU(N)$ gauge theory which spontaneously breaks global $Z(N)$ invariance. At temperatures $T < T_d$, the $Z(N)$ global symmetry associated with confinement is unbroken. The standard equilibrium order parameter for $Z(N)$ symmetry breaking is the Polyakov loop L, defined in equilibrium as the path-ordered exponential

$$L(\overrightarrow{x}) = P \exp\left[i \int_0^{1/T} dt \, A_0(\overrightarrow{x}, t)\right] \tag{1.1}$$

The Polyakov loop can be defined for a general density matrix by its association with the projection operator onto gauge invariant states. [3] Because of $Z(N)$ symmetry, $\langle L_F \rangle = \frac{1}{N} \langle Tr_F(L) \rangle$ vanishes below T_d. When the temperature is rapidly increased to $T > T_d$,

$\langle L_F \rangle = 0$ is no longer the stable state of the system, and must evolve to a new equilibrium state with $\langle L_F \rangle \neq 0$, reflecting the transition to the gluon plasma phase. We will use the Polyakov loop as the primary tool for the study of this process.

II. EFFECTIVE POTENTIAL

The instability of $\langle L_F \rangle = 0$ at high temperatures follows from the one-loop finite temperature effective potential for the Polyakov loop, as derived by Gross, Pisarski and Yaffe and Weiss. [4] [5] For simplicity, consider the case of $SU(2)$. At any spacetime point, the Polyakov loop can be diagonalized, and we can write

$$L = \begin{pmatrix} e^{i\pi q} & \\ & e^{-i\pi q} \end{pmatrix}. \tag{2.1}$$

where $0 \leq q \leq 1$. It is convenient to introduce the parameter ψ, which is related to q by $q = (1 - \psi)/2$. The order parameter L_F is given by

$$L_F = \frac{1}{2} Tr_F L = \cos\left[\pi\left(1 - \psi\right)/2\right]. \tag{2.2}$$

The effective potential at one loop for gauge bosons in a constant Polyakov loop background is

$$V(\psi) = -\frac{\pi^2 T^4}{15} + \frac{\pi^2 T^4}{12}\left(1 - \psi^2\right)^2. \tag{2.3}$$

The one loop result dominates the effective potential for $T \gg \Lambda_{QCD}$ due to asymptotic freedom. The first term is the standard black body result, obtained when $\psi = 1$. Figure 1 shows V as a function of ψ, normalized such that $V(\psi = 1) = 0$. The use of the variable ψ makes the $Z(2)$ symmetry of the potential under $\psi \to -\psi$ manifest. Note that the equilibrium value of ψ is ± 1, corresponding to $L_F = \pm 1$; $\psi = 0$, corresponding to $L_F = 0$, is a maximum of $V(\psi)$.

Our picture of the quenching process is that the system is initially in a state where ψ is equal to zero at some temperature below T_d. When the system is quickly raised to a new

3

temperature $T > T_d$, the system is still in the state with $\psi = 0$. However, the system is unstable, and must eventually find its way to either $\psi = +1$ or $\psi = -1$. Because we quench into a region of the phase diagram where $V''(\psi) < 0$, the system will decay to the equilibrium state via spinodal decomposition.

III. LANGEVIN MODEL

In order to study the dynamics of this transition, we use the effective action of Bhattacharya combined with Langevin dynamics. [6] The effective action takes the form

$$S_{eff}[\psi] = \int d^3x \left[\frac{\pi^2 T}{2g^2} (\nabla \psi)^2 + \frac{\pi^2 T^3}{12} \left(1 - \psi^2\right)^2 \right]. \tag{3.1}$$

The equilibrium distribution will be

$$\exp\left[-S_{eff}[\psi]\right]. \tag{3.2}$$

We postulate Langevin dynamics of the form

$$\frac{\partial \psi(x,\tau)}{\partial \tau} = -\Gamma \frac{\delta S_{eff}[\psi]}{\delta \psi(x,\tau)} + \eta(x,t) \tag{3.3}$$

where the white noise η is normalized to

$$\langle \eta(x,\tau)\eta(x',\tau') \rangle = 2\Gamma \delta^3(x - x')\delta(\tau - \tau'). \tag{3.4}$$

Assuming translation-invariant initial conditions, the expectation value $\Psi(\tau) = \langle \psi(x,\tau) \rangle$ will evolve away from the unstable value $\Psi = 0$ approximately as

$$\frac{d\Psi}{d\tau} = \Gamma \frac{\pi^2 T^3}{3} \left(1 - \Psi^2\right) \Psi \tag{3.5}$$

This gives initial exponential growth, which slows down as equilibrium is approached.

The late-time relaxational behavior of ψ is controlled by the Debye screening mass m_D, given by $m_D^2 = 2g^2 T^2/3$. Near equilibrium, any effects of initial conditions decay exponentially as $\exp\left[-\frac{2\pi^2 \Gamma T}{g^2}(k^2 + m_D^2)\tau\right]$. However, for early times, the initial conditions contribute to $\left\langle \widetilde{\psi}(k,\tau)\widetilde{\psi}(-k,\tau) \right\rangle$ a term of the form

4

$$\widetilde{\psi}(k,0)\widetilde{\psi}(-k,0)\exp\left[-\frac{2\pi^2\,\Gamma T}{g^2}(k^2-k_c^2)\tau\right] \tag{3.6}$$

where $k_c^2 = g^2T^2/3 = m_D^2/2$. Modes with $k < k_c$ are initially not damped but grow exponentially, with the $k = 0$ mode growing the fastest. This is a characteristic feature of spinodal decomposition with a non-conserved order parameter.

Because pure $SU(2)$ gauge theory has a second-order deconfining transition, spinodal decomposition will occur after quenching to any temperature $T > T_d$. The situation is more subtle for $SU(3)$. The one-loop effective potential is unstable at $L_F = 0$. For temperatures sufficiently large that the one-loop effective potential for L is reliable, spinodal decomposition will occur. However, the first-order character of the pure $SU(3)$ transition implies the existence of a metastable phase with $\langle L_F \rangle = 0$ for some range of temperature $T \gtrsim T_d$. This in turn implies that nucleation followed by bubble growth is the important mechanism for attaining equilibrium for some range of temperatures just above T_d.

IV. DYNAMICAL QUARKS

When dynamical particles in the fundamental representation, e.g, quarks, are included, the $Z(N)$ symmetry is explicitly broken. At low temperatures, $L_F(x) \neq 0$. However, after a rapid quench to $T > T_d$, L_F must still change to its new equilibrium value. This change may involve spinodal decomposition or nucleation as well as relaxational processes. The relevant potential for $SU(2)$ with N_f massless fermion flavors has the form

$$V(\psi) = \frac{\pi^2 T^4}{12}\left(1-\psi^2\right)^2 + \frac{N_f\,\pi^2 T^4}{96}\left(7+2\psi-\psi^2\right)\left(1-\psi\right)^2. \tag{4.1}$$

With $N_f = 2$, $V''(\psi)$ is negative for $\psi < \frac{1}{3}$, as shown in figure 2, so spinodal decomposition will take place for a significant range of initial conditions. [4] [5] Thus the initial value of L_F in the confined phase will determine whether spinodal decomposition occurs. These considerations are independent of any static critical behavior, *e.g.*, the existence of a deconfinement or chiral phase transition for particular values of quark parameters. Because $Z(N)$

symmetry breaking terms in the effective potential vanish in the limit of infinite quark mass, spinodal decomposition is to be expected for sufficiently large quark masses.

V. MONTE CARLO RESULTS FOR $SU(2)$

We have tested these theoretical ideas with simulations of rapidly quenched pure $SU(2)$ gauge theory. Lattices of size $32^3 \times 4$ and $64^3 \times 4$ were equilibrated at $\beta = 2.0$; the deconfinement transition for $N_t = 4$ occurs at $\beta_d = 2.2986 \pm 0.0006$. [7] The coupling constant was increased instantaneously to $\beta = 3.0$, and the approach to equilibrium monitored via the Polyakov loop and other observables. For simplicity, the heat bath algorithm was used both for equilibration at low temperature before the quench and for subsequent dynamical evolution after the quench. While this time evolution is of course not the true time evolution of the non-equilibrium quantum field theory, features such as spinodal decomposition which depend only on the equilibrium effective action will occur with any local updating algorithm which converges to the equilibrium distribution. The abrupt change in β is a potential cause of concern with this procedure, since the lattice spacing, and hence the physical volume, changes in all directions when β is changed. However, the large spatial sizes used should mitigate this effect. It is also possible to maintain a constant spatial volume with anisotropic lattice couplings. As an alternative, we have also taken $32^3 \times 4$ sections from $32^3 \times 10$ configurations equilibrated at $\beta = 3.0$, with similar results. However, the initial configurations produced in this way suffer from an obvious problem due to abrupt joining of the new boundaries in the time direction.

In figure 3, we show the Polyakov loop expectation value versus Monte Carlo time for one $64^3 \times 4$ simulation. Comparison with a numerical integration of equation 3.5 shows qualitative agreement, although the equilibrium value of $\langle L_F \rangle$ measured in simulations has a multiplicative renormalization. Figure 4 shows the Fourier transform of the connected Polyakov two point function $S(k, \tau)$ for low values of the wave number as a function of Monte Carlo time for the same simulation. Note the early exponential rise in these modes, followed

by a sharp disappearance as the Polyakov loop reaches its equilibrium value, characteristic of spinodal decomposition. Only the low momentum modes exhibit this growth; above k_c no such growth occurs. Although the general behavior of $S(k, \tau)$ is the same for each run, many details are run dependent. In this particular run, the $k/T = 0.68$ mode achieves a larger amplitude than $k/T = 0.56$, which is atypical. In some runs, there is clear evidence for mode-mode coupling, reflecting the nonlinearity of the system. For each run, we have estimated the rate of growth of each low-momentum mode by fitting $log(S(k, \tau))$ to a straight line in τ for early times. We can extract k_c as the value where the growth rate is zero. From equation 3.6, the growth rate of each line is proportional to $k_c^2 - k^2$ for the linearized theory, but this may not represent the true time evolution. In any case, the growth rates measured in each run are highly dependent on initial conditions. In figure 5, we plot these growth rates versus k^2/T^2 for the same run used in figure 4. The error bars are naive estimates of the error for each growth rate for this particular run. The x intercept provides an estimate of k_c^2 for each run. Using multiple 64^3 runs at $\beta = 3.0$, we have estimated k_c/T to be 1.09 ± 0.08. The principle errors in this estimate come from the sensitivity of individual modes to initial conditions and the discrete character of k on the lattice. We can compare this with lattice measurements of the Debye screening length, assuming the one-loop relation

$$\frac{k_c}{T} = \frac{m_D(T)}{\sqrt{2}T} \tag{5.1}$$

holds in general. Using the results of Heller *et al.* [8] for $m_D(T)$, we obtain $k_c/T = 1.35(5)$. We consider this to be reasonable agreement, given the many uncertainties involved.

Somewhat less sensitive to initial conditions is the traditional observable k^*, which is defined to be

$$k^*(\tau) = \frac{\int_0^\infty dk \; k \, S(k, \tau)}{\int_0^\infty dk \; S(k, \tau)}. \tag{5.2}$$

It is convenient to plot $T/k^*(\tau)$ versus τ, as in figure 6. Its early time behavior is predicted from equation 3.6 to be $1/k^*(\tau) \sim \sqrt{\tau}$, typical of length scales in diffusive processes. We do observe this behavior, but only for very early times; on $64^3 \times 4$ lattices, this occurs for

$0 \leq \tau \lesssim 120$. For the run shown in figure 6, $T/k^*(\tau)$ is fit well by $a\tau^p$ for $0 \leq \tau \leq 120$, where $p = 0.54 \pm 0.03$.

VI. CONCLUSIONS

As we have shown above, theoretical and simulation results both indicate the relevance of spinodal decomposition in the equilibration of a gluon plasma after a rapid quench to high temperature. Since simulations and theoretical analysis were both carried out in Euclidean space, the significance of these results for experiment is not clear. However, spinodal decomposition is a general phenomenon whenever a system is in an unstable initial state, as determined by some local variable. Since we have considered a rapid heating of a finite temperature gauge theory, it is natural to ask what happens when rapid cooling takes place, as might occur in the late stages of the expansion of a quark-gluon plasma, or in the early universe. At low temperatures, we expect that $V(\psi)$ has a single minimum and $V''(\psi) > 0$ everywhere; this is required by $Z(N)$ symmetry in the case of a pure gauge theory. Thus theory predicts the absence of unstable modes, and that relaxational processes should dominate the approach to equilibrium. We have performed simulations of such a cooling process, in which $32^3 \times 4$ lattice configurations equilibrated at $\beta = 3.0$ are suddenly cooled to $\beta = 2.0$. Examination of the data from these runs shows no sign of spinodal decomposition.

It is interesting to contrast the phenomenon of spinodal decomposition in a rapid heating with the formation of a disordered chiral condensate (DCC) in a rapid cooling. [9] In both cases, exponentially growing low-momentum modes occur when an unstable initial state must equilibrate to a final state associated with a broken symmetry. In the case of a DCC, chiral symmetry is the relevant symmetry. For massless quarks, the symmetry is spontaneously broken at low temperatures. With sufficiently light quarks, the overall structure of the potential survives, and the approach to equilibrium is fundamentally the same as the case of massless quarks. In the absence of fundamental representation particles such as quarks, $Z(N)$ symmetry breaks spontaneously at high temperatures. Provided there are sufficiently

few light quarks, spinodal decomposition still occurs at sufficiently high temperature.

Just as the formation of a DCC may lead to enhanced production of low-momentum pions, spinodal decomposition should lead to enhanced production of low-momentum gluons in the early stages of plasma formation. The characteristic scale for such a phenomenon would be gT. As the system equilibrates, this enhancement of the small-k part of the gluon distribution will be eliminated. It is interesting to note that another, perhaps related, mechanism for the creation of exponentially growing low-momentum modes has been proposed; it has been argued that such instabilities can significantly affect the temporal evolution of the system. [10]

In contrast to the $SU(2)$ results presented here, the case of $SU(3)$ presents additional complications due to the presence of the confined phase as a metastable state over some range of temperature in the deconfining regime. Study of the $SU(3)$ dynamics may be helpful in exploring the limits of metastability. It would also be of interest to study via simulation the effect of unquenched quarks on the dynamics. Because the dynamic part of the simulation is much faster than creating equilibrated field configurations, this could be done fairly easily if large equilibrated unquenched lattice field configurations became available.

REFERENCES

[1] J. Gunton and M. Droz, Introduction to the Theory of Metastable and Unstable States, Springer-Verlag, Berlin (1983).

[2] P. Chaikin and T. Lubensky, Principles of Condensed Matter Physics, Cambridge University Press, Cambridge (1995).

[3] T. Banks and A. Ukawa, Nucl. Phys. B225, 145 (1983).

[4] D. Gross, R. Pisarski and L. Yaffe, Rev. Mod. Phys. 53, 43 (1981).

[5] N. Weiss, Phys. Rev. D **24**, 475 (1981); Phys. Rev. D **25**, 2667 (1982).

[6] T. Bhattacharya, A. Gocksch, C. Korthals Altes and R. Pisarski, Phys. Rev. Lett. 66, 998 (1991); Nucl. Phys. B383, 497 (1992).

[7] J. Fingberg, U. Heller and F. Karsch, Nucl. Phys. B392, 493 (1993).

[8] U. Heller, F. Karsch and J. Rank, Phys. Rev. D57, 1438 (1998).

[9] K. Kowalski, J. Bjorken and C. Taylor, SLAC-PUB-6109 (1993); K. Rajagopal and F. Wilczek, Nucl. Phys. B399, 395 (1993); Nucl. Phys. B404, 577 (1993).

[10] S. Mrowczynski, Phys. Lett. B314, 118 (1993); Phys. Rev. C49, 2191 (1994); Phys. Lett. B393, 26 (1997); S. Mrowczynski and M. Thoma, hep-ph/0001164.

FIG. 1.   The effective potential $V(\psi)/T^4$ for $SU(2)$ with $N_f = 0$ as a function of ψ.
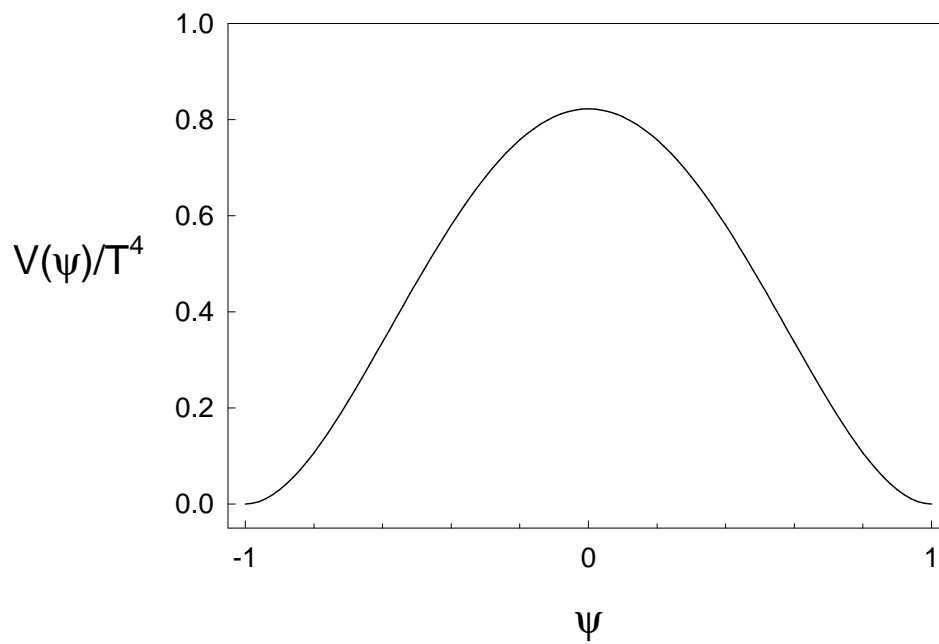
FIG. 2. The effective potential $V(\psi)/T^4$ for $SU(2)$ with $N_f = 2$ as a function of ψ.
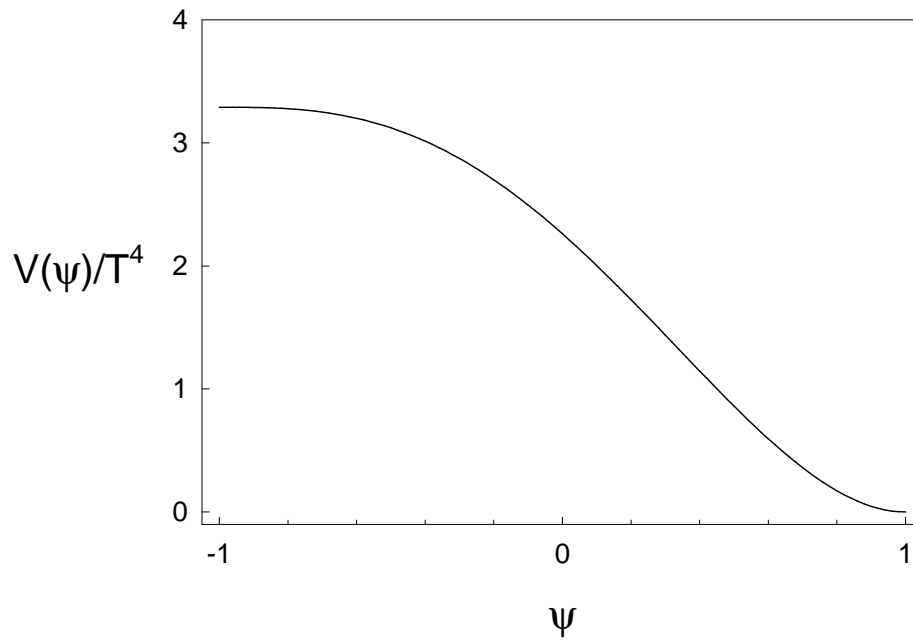
FIG. 3.   Polyakov loop as a function of Monte Carlo time.
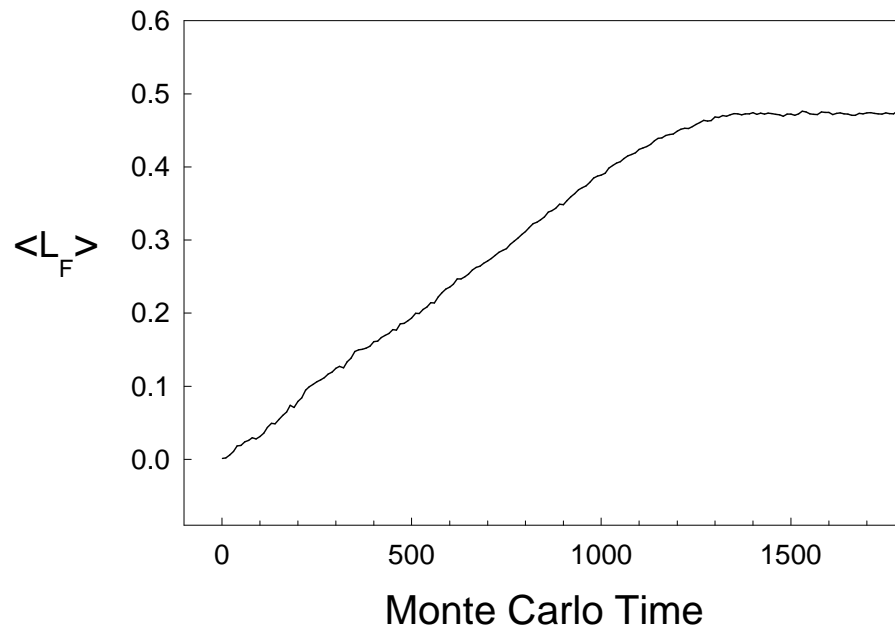
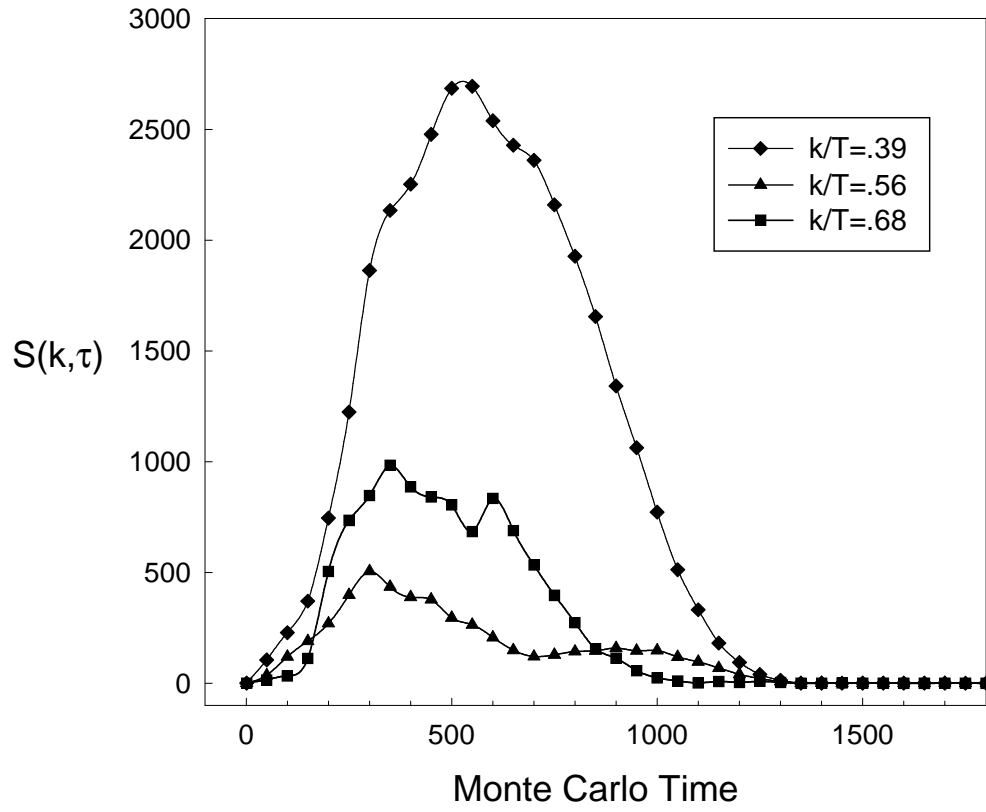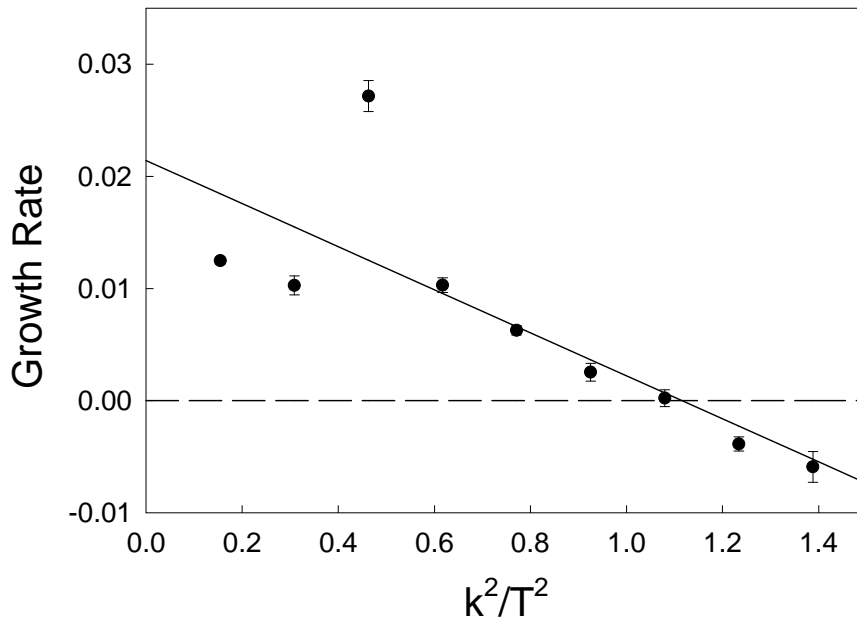FIG. 4. $S(k, \tau)$ versus Monte Carlo time.

FIG. 5. Growth rate of $S(k, \tau)$ versus k^2/T^2.

FIG. 6. $T/k^*(\tau)$ versus Monte Carlo time.